Evaluation of DSP-Based PID and Fuzzy Controllers for DC–DC Converters

Liping Guo, *Member, IEEE*, John Y. Hung, *Senior Member, IEEE*, and R. M. Nelms, *Fellow, IEEE*

***Abstract*—In this paper, digital proportional–integral–derivative (PID)-type and fuzzy-type controllers are compared for application to the buck and boost dc–dc converters. Comparison between the two controllers is made with regard to design methodology, implementation issues, and experimentally measured performance. Design of fuzzy controllers is based on heuristic knowledge of converter behavior, and tuning requires some expertise to minimize unproductive trial and error. The design of PID control is based on the frequency response of the dc–dc converter. Implementation of linear controllers on a digital signal processor is straightforward, but realization of fuzzy controllers increases computational burden and memory requirements. For the boost converter, the performance of the fuzzy controller was superior in some respects to that of the PID controllers. The fuzzy controller was able to achieve faster transient response in most tests, had a more stable steady-state response, and was more robust under some operating conditions. In the case of the buck converter, the fuzzy controller and PID controller yielded comparable performances.**

***Index Terms*—Boost converter, buck converter, digital control, digital signal processor (DSP), fuzzy control, proportional–integral–derivative (PID) control.**

I. Introduction

PROPORTIONAL–INTEGRAL–DERIVATIVE (PID) control and fuzzy control are two different control approaches for dc–dc converters. Fuzzy control is a type of nonlinear control, while PID control is a traditional linear control method used in many applications. Linear PID controllers for dc–dc converters are usually designed by classical frequency response techniques applied to the small-signal models of converters [1]. A Bode plot is adjusted in the design to obtain the desired loop gain, crossover frequency, and phase margin. Alternatively, the transient response can be tuned using root locus-type approaches [2]. The stability of the system is guaranteed by an adequate phase margin. PID control is typically designed for one nominal operating point, but a dc–dc converter's small-signal model changes with variations in the operating point [3]. For a buck converter, the magnitude of the frequency response depends on the duty cycle. Duty cycle variations do not change the shape of the magnitude plot of the transfer function, but only shift the plot upward or downward. For a boost converter, both poles and a right-half-plane zero are dependent on the duty cycle, so the Bode plots can exhibit significant variation. Therefore, a PID controller may not respond well to significant changes in operating points.

Design of fuzzy controllers is based on expert knowledge of the plant instead of a precise mathematical model [4]. Controllers based on fuzzy logic have been applied to a broad range of engineering problems [5], particularly those having nonlinear dynamics. Fuzzy logic controller have recently been implemented as embedded controllers for robotics [6] and renewable energy systems [7], [8]. Numerous motor drive problems have been solved using fuzzy principles [9]–[12]. As digital signal processing technologies have increased in computing power and speed, researchers have recently applied fuzzy principles to power electronic systems [13]. Fuzzy controllers can be designed to adapt to the nonlinear properties of dc–dc converters under varying operating conditions [14]. Researchers have also proposed to blend fuzzy logic concepts with other control methods, including sliding-mode control [15], [16]. Approximation of fuzzy rule-based control has also proven effective compared to traditional linear control [17].

In this paper, PID control and fuzzy control are compared in the aspects of design, implementation, and performance. Two sections of the paper are devoted to explaining the design methods. Section III describes the linear system design methods used with the buck and boost converters. Fuzzy controller design is detailed in Section IV. The authors believe the material in these two sections will help readers understand the differences between the linear and fuzzy design approaches. These design descriptions are preceded by Section II, where the models that support linear system design are developed. Implementation and experimental results for a buck converter and a boost converter using the two different control methods are reported and compared in Sections V and VI.

II. Small-Signal Models

Linear controllers for dc–dc converters are often designed based on mathematical models. To achieve a certain performance objective, an accurate model is essential. A number of ac equivalent circuit modeling techniques have appeared in the literature, including circuit averaging, averaged switch modeling, the current injected approach, and the state-space averaging method [18]. Among these methods, the state-space averaged modeling is most widely used to model dc–dc converters. In this section, the basic models are reviewed, and experimental circuit parameters are presented.

Manuscript received December 5, 2007; revised February 24, 2009. First published March 16, 2009; current version published June 3, 2009. This work was supported by the Center for Space Power and Advanced Electronics with funds from NASA Grant NCC3-511, Auburn University, and the Center's industrial partners.

L. Guo is with the Department of Technology, Northern Illinois University, DeKalb, IL 60115 USA (e-mail: lguo@niu.edu).

J. Y. Hung and R. M. Nelms are with the Department of Electrical and Computer Engineering, Auburn University, Auburn, AL 36849-5201 USA (e-mail: j.y.hung@ieee.org; nelmsrm@auburn.edu).

Digital Object Identifier 10.1109/TIE.2009.2016955

TABLE I
CIRCUIT PARAMETERS OF THE PROTOTYPE BUCK CONVERTER

Parameter	Value	Units
Filter capacitance, C	1000	μF
Filter inductance, L	150	μH
Load resistance, R	10	Ω
ESR of capacitor, R_C	30	mΩ
ESR of inductor, R_L	10	mΩ

A. Buck Converter's Small-Signal Model

A buck converter's small-signal control-to-output transfer function, derived by the standard state-space averaging technique, is given by (1). In this transfer function, V_o is the output voltage, D is the duty cycle, C is the output capacitance, L is the inductance, and R is the load resistance. Parameters R_C and R_L are the equivalent series resistance (ESR) of C and L, respectively,

$$\frac{\hat{v}_\mathrm{o}(s)}{\hat{d}(s)} = \frac{V_\mathrm{o}}{D}\left(\frac{1+sR_\mathrm{C}C}{1+a_1 s+a_2 s^2}\right) \tag{1}$$

where

$$a_1 = R_\mathrm{C}C + (R\|R_\mathrm{L})C + \frac{L}{R+R_\mathrm{L}}$$
$$a_2 = \frac{R+R_\mathrm{C}}{R+R_\mathrm{L}}LC.$$

The buck converter transfer function is a second-order low-pass filter, with a left-half-plane zero introduced by the ESR of the filter capacitance [3]. The cutoff frequency of the low-pass filter is $\omega_\mathrm{c} = 1/\sqrt{LC}$. The magnitude of the transfer function depends on the duty cycle D. Variations of D do not change the shape of the frequency response, but only shift the magnitude plot upward or downward. The prototype buck converter's nominal operating point is as follows: $V_\mathrm{in} = 20$ V, $V_\mathrm{o} = 12$ V, and $D = 0.6$. Values of the circuit parameters of the prototype buck converter are listed in Table I. The transfer function at the nominal operating point is given by

$$\frac{\hat{v}_\mathrm{o}(s)}{\hat{d}(s)} = \frac{6\times10^{-4}s+20}{1.503\times10^{-7}s^2+5.4975\times10^{-5}s+1}. \tag{2}$$

The model has complex conjugate poles at $615.9 \pm j2481.5$, which causes a 180° phase delay at the approximate frequency of 2500 rad/s (400 Hz). The model also has a zero at 33 333 rad/s (5.3 kHz). Frequency response data for all of the experimental circuits was measured using an analog network analyzer (AP Instruments Model 102B). The measured frequency response of the buck converter is shown in Fig. 1. The measured frequency response compares favorably with the theoretical model, particularly below the 20-kHz switching frequency, so a linear controller can be designed based on (2). Above 20 kHz, switching frequency noise introduces greater uncertainty in the experimental data, particularly in the phase plot.

B. Boost Converter's Small-Signal Model

The control-to-output small-signal transfer function of a boost converter, obtained using standard state-space averaging techniques, is shown in (3). In this equation, D is the nominal duty cycle, $L_e = L/(1-D)^2$, and $D_0 = 1-D$

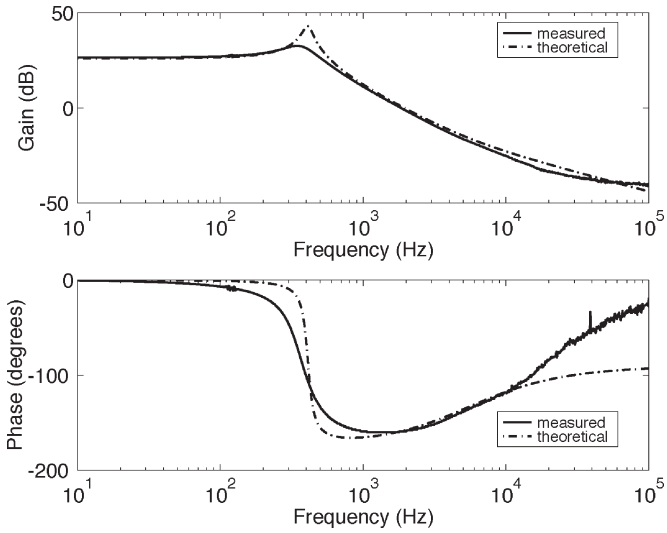

Fig. 1. Measured and theoretical frequency responses of the buck converter.

$$\frac{\hat{v}_\mathrm{o}(s)}{\hat{d}(s)} = \frac{V_\mathrm{o}}{D_0 L_e C}\frac{(1-sL_e/R)(sR_\mathrm{C}C+R_\mathrm{C}/R+1)}{s^2+b_1 s+b_2} \tag{3}$$

where

$$b_1 = \frac{\left(R_\mathrm{L}/D_0^2\right)+\left(R_\mathrm{C}/D_0\right)}{L_e} + \frac{1}{RC}$$
$$b_2 = \frac{\left(R_\mathrm{L}/D_0^2\right)+\left(R_\mathrm{C}/D_0\right)}{RL_eC} + \frac{1}{L_eC}.$$

The transfer function (3) is a second-order low-pass filter with two zeros. The low-pass filter's cutoff frequency is given by (4). The zero in the left half-plane is shown in (5), and the zero in the right half-plane is shown in

$$\omega_\mathrm{C} = \frac{1-D}{\sqrt{LC}} \tag{4}$$

$$\omega_\mathrm{zl} = -\frac{1+R_\mathrm{C}/R}{R_\mathrm{C}C} \tag{5}$$

$$\omega_\mathrm{zr} = (1-D)^2\frac{R}{L}. \tag{6}$$

The cutoff frequency ω_c and right-half-plane zero ω_zr are functions of nominal duty cycle D. In a closed-loop voltage-control system, the filter element will change as the duty cycle changes, which means the transfer function will change accordingly. The boost converter under feedback control is a nonlinear function of the duty cycle [3], which makes controller design for the boost converter much more challenging than that for the buck converter from the viewpoint of stability and bandwidth.

For the experimental boost converter utilized in this effort, the input voltage $V_\mathrm{in} = 5$ V, the output voltage $V_\mathrm{o} = 12$ V, and the nominal duty cycle $D = 0.58$. Circuit parameters of the prototype boost converter are listed in Table II. There is a clear discrepancy between the theoretical model and the

TABLE II
CIRCUIT PARAMETERS OF THE PROTOTYPE BOOST CONVERTER

Parameter	Value	Units
Filter capacitance, C	1056	μF
Filter inductance, L	250	μH
Load resistance, R	25	Ω
ESR of capacitor, R_C	30	mΩ
ESR of inductor, R_L	10	mΩ

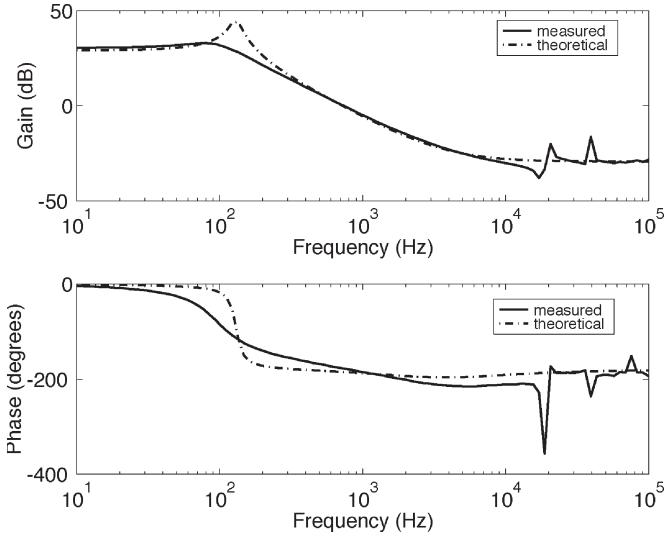

Fig. 2. Measured and theoretical frequency responses of the boost converter.

measured frequency response, as shown in Fig. 2. Part of the discrepancy is because there is more damping in the actual plant than in the theoretical model. The circuit elements including the inductor, capacitor, and the switching devices in a boost converter are not ideal. In addition, the nonlinear property of the boost converter's small-signal model may also cause the discrepancy. Effects of the 20-kHz switching also contribute to uncertainty in the high-frequency response.

By fitting the experimental frequency response data using MATLAB, a transfer function for the boost converter was constructed, as shown in (7). The measured transfer function has two zeros at -5.961×10^4 and 1.468×10^4 rad/s, and two complex conjugate poles at $-412.6 \pm j610$ rad/s

$$\frac{\hat{v}_{\rm o}(s)}{\hat{d}(s)} = \frac{-5.6956 \times 10^{-3} s^2 - 2.5589 \times 10^2 s + 4.9831 \times 10^6}{s^2 + 8.2525 \times 10^2 s + 5.4241 \times 10^5}. \tag{7}$$

III. DESIGN OF PID CONTROL FOR DC–DC CONVERTERS

Both PID and PI controllers were designed for the buck and the boost converters for operation during a startup transient and steady state, respectively. The derivative term in the PID controller is susceptible to noise and measurement error of the system, which can cause oscillation in the duty cycle and voltage during steady state conditions. However, during a transient, the derivative term is needed to reduce the settling time by predicting the changes in error. In this implementation, the PID controller is employed during transient conditions, and the PI controller is utilized under steady-state conditions [19].

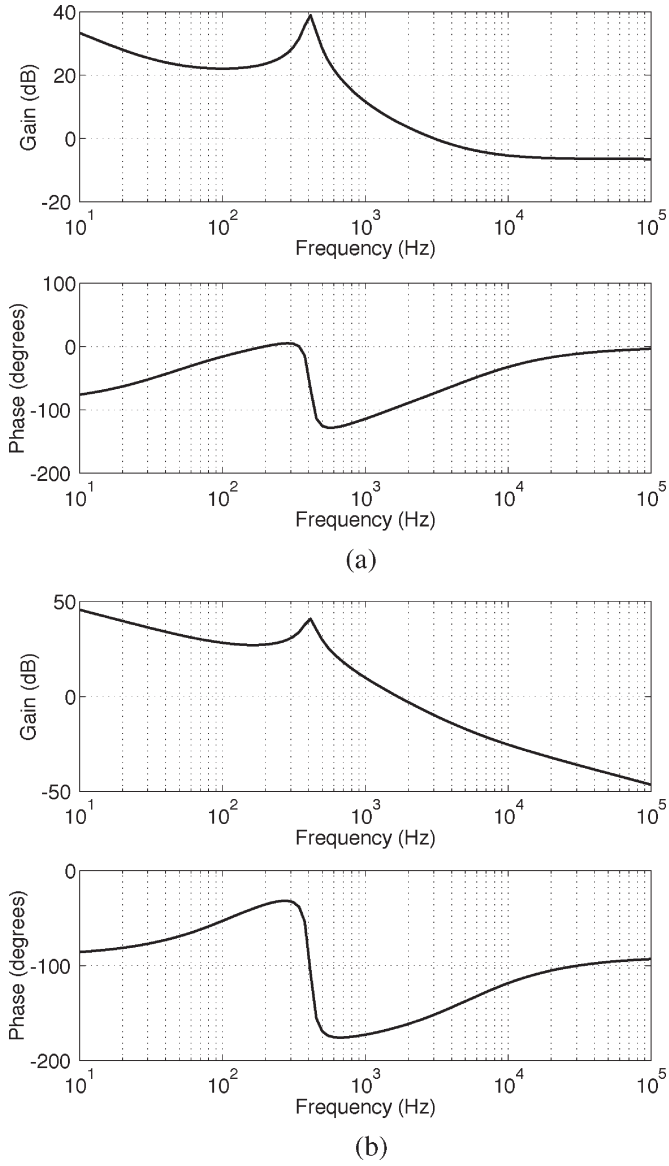

Fig. 3. Frequency responses of linearly compensated buck converter. (a) With PID controller. (b) With PI controller.

A. Design of PID and PI Control for a Buck Converter

A PID controller was designed for the buck converter to improve the loop gain, crossover frequency, and phase margin. One zero was placed an octave below the cutoff frequency (approximately 260 rad/s) and the other one at 4.6×10^3 rad/s. The transfer function of the PID controller is given by

$$G_{\rm C}(s) = 0.5786 + \frac{142.4}{s} + 1.19 \times 10^{-4} s. \tag{8}$$

The Bode plot for the compensated system is shown in Fig. 3(a). As shown in this plot, the gain at low frequency is high, the phase margin is 107° at a gain crossover frequency approximately 3 kHz.

A PI controller was also designed for the buck converter to reduce steady-state oscillation. One pole was placed at the origin, and one zero was placed at 800 rad/s. The dc gain of the controller was adjusted to obtain sufficient phase margin

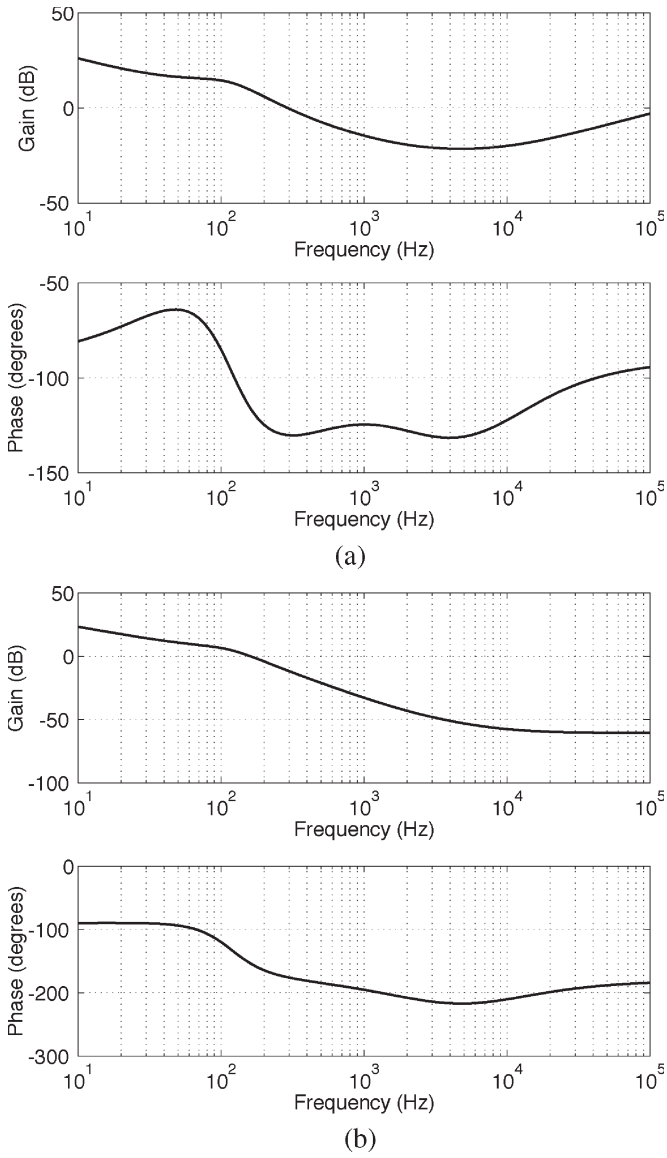

Fig. 4. Frequency responses of linearly compensated boost converter. (a) With PID controller. (b) With PI controller.

and high crossover frequency. The transfer function of the PI controller is given by

$$G_{\mathrm{C}}(s) = 0.75 + \frac{600}{s}. \tag{9}$$

The Bode plot for the PI compensated system is shown in Fig. 3(b) and shows that the phase margin is 15.4° at gain crossover frequency approximately 1.7 kHz.

B. Design of PID and PI Control for a Boost Converter

The PID and PI controllers were designed based on the measured small-signal model of the boost converter in (7) using frequency response techniques. One zero of the PID controller was placed at 260 rad/s, and the other zero was placed at 2600 rad/s. The transfer function of the PID controller is shown in (10). The Bode plot of the PID-compensated boost converter is shown in Fig. 4(a). The gain crossover frequency of the PID-compensated system is approximately 290 Hz, and the phase margin is 50°

$$G_{\mathrm{C}}(s) = 0.567 + \frac{134.13}{s} + 1.98 \times 10^{-4} s. \tag{10}$$

For the PI controller, a pole was placed at the origin, and a zero was placed at 600 rad/s. The transfer function of the PI controller is shown in (11). The Bode plot of the PI-controller-compensated system is shown in Fig. 4(b). The gain crossover frequency of the PI-compensated system is approximately 160 Hz, and the phase margin is 26.3°

$$G_{\mathrm{C}}(s) = 0.1667 + \frac{100}{s}. \tag{11}$$

IV. Design of Fuzzy Control for DC–DC Converters

Fuzzy systems can be considered a type of nonlinear function interpolator [17]. The design of fuzzy controllers does not require an exact mathematical model. Instead, they are designed based on general knowledge of the plant. Fuzzy controllers can be designed to adapt to varying operating points. A fuzzy controller contains four main components: 1) the fuzzification interface that converts its input into information that the inference mechanism can use to activate and apply rules; 2) the rule base that contains the expert's linguistic description of how to achieve good control; 3) the inference mechanism that evaluates which control rules are relevant in the current situation; and 4) the defuzzification interface that converts the conclusion from the inference mechanism into the control input to the plant [4]. There are two inputs for the fuzzy controller for the buck and boost converters. The first input is the error in the output voltage given by (12), where $ADC[k]$ is the converted digital value of the kth sample of the output voltage and Ref is the digital value corresponding to the desired output voltage. The second input is the difference between successive errors and is given by

$$e[k] = Ref - ADC[k] \tag{12}$$

$$ce[k] = e[k] - e[k-1]. \tag{13}$$

The two inputs are multiplied by the scaling factors g_0 and g_1, respectively, and then fed into the fuzzy controller. The output of the fuzzy controller is the change in duty cycle $\Delta d[k]$, which is scaled by a linear gain h. The scaling factors g_0, g_1, and h can be tuned to obtain a satisfactory response.

A. Two Methods for Computing the Commanded Duty Cycle

There are two methods to calculate the new duty cycle from the fuzzy controller's output $\Delta d[k]$. A block diagram model of the first method is shown in Fig. 5(a). In this method, the fuzzy controller output $\Delta d[k]$ is scaled by the output gain h, and then added to the previous sampling period's duty cycle $d[k-1]$

$$d[k] = d[k-1] + h\Delta d[k]. \tag{14}$$

The first method (14) represents a discrete time integration of the fuzzy controller output. Integrating the fuzzy controller's

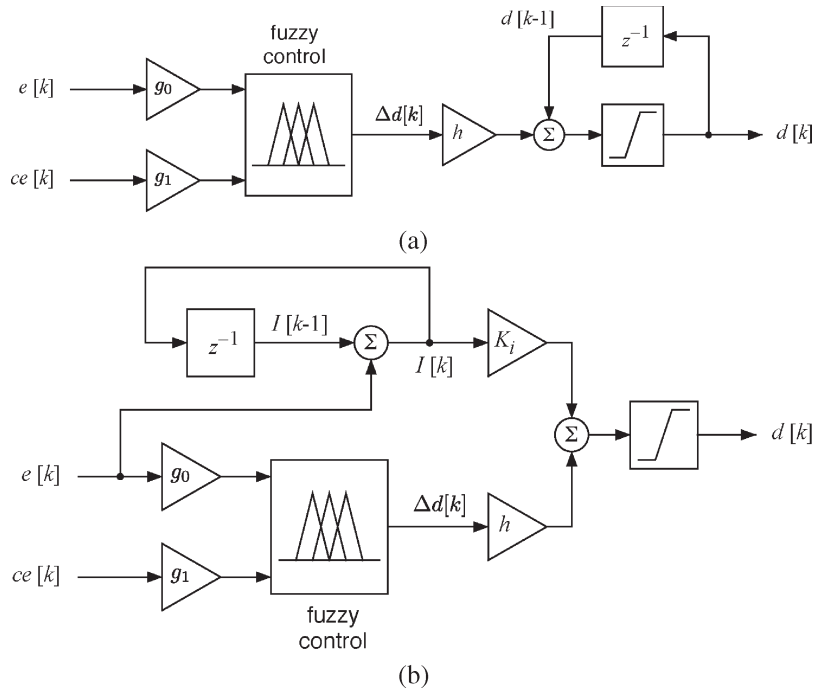

Fig. 5. Two methods of duty cycle calculation. (a) Method (14). (b) Method (15).

output increases the system type and reduces steady-state error.

The second method of computing the new duty cycle is shown in Fig. 5(b). The fuzzy controller's output is scaled by h, and then added to the output of a parallel integrator

$$d[k] = K_i I[k] + h\Delta d[k]. \tag{15}$$

Here, $I[k]$ is the output of the discrete time integration of the error $e[k]$, and K_i is the gain of the integrator. The integrator is used to eliminate steady-state error.

In the first structure of the fuzzy controller, an integrator is in series with the fuzzy logic controller, while in the second structure, the integrator is in parallel with the fuzzy logic controller. A disadvantage of the first structure is that the output gain h has to be tuned to very small values to avoid voltage oscillations in steady state. On the other hand, a very small output gain h tends to slow down the transient response time because more sampling periods are needed to arrive at the desired duty cycle. In the second structure, the change of duty cycle is not accumulated every sampling period, so the output gain h can be increased to reduce transient response time. The second structure is a combination of linear and nonlinear controllers. In the literature, the first method in Fig. 5(a) is more prevalent than the second method in Fig. 5(b) [12], [20], [21]. In this paper, only the second method is applied to the buck converter to obtain satisfactory response, while for the boost converter, a combination of the methods is applied to get the desired response. The second structure is applied during startup transient to obtain fast transient response, and the first structure is applied during steady state in order to obtain stable steady-state response and to reduce steady-state error. For both methods, the duty cycle $d[k]$ was limited to be between 10% and 90% for the buck converter, and further limited to be between 20% and 80% for the boost converter.

B. Fuzzification

The first step in the design of a fuzzy logic controller is to define membership functions for the inputs. Each universe of discourse is divided into fuzzy subsets. For purposes of implementation, the computation time and code size of the fuzzy controller can be reduced when the number of subsets for the positive and negative parts is a power of two, because shift instructions can be used to calculate the membership degrees instead of division functions. There are 17 fuzzy subsets in the fuzzy controller for the buck converter: $\{N8, N7, \ldots, Z, \ldots, P7, P8\}$, where N indicates negative, Z represents zero, and P indicates positive. Of the 17 subsets, there were eight subsets for the positive and negative parts of the universe of discourse, respectively. The variables $\mu_e(e[k])$ and $\mu_{ce}(ce[k])$ are the membership degrees assigned to each fuzzy subset to quantify the certainty that the input can be classified linguistically into the corresponding fuzzy subsets. For the boost converter, each universe of discourse is divided into 33 fuzzy subsets: $\{N16, N15, \ldots, N1, Z, P1, \ldots, P15, P16\}$. There were 16 fuzzy subsets in the negative and positive parts of the universe of discourse in order to reduce the computation time. The number of fuzzy subsets was determined based on the experimental results of buck and boost converters. 17 fuzzy subsets for the buck converter and 33 fuzzy subsets for the boost converter were the smallest number of fuzzy subsets that yielded satisfactory results.

There are tradeoffs when selecting the number of fuzzy subsets, as well as the shape of membership functions. There has been significant research into the impact of membership function shape on control system performance [22], [23]. Triangular

membership functions are used in this paper to minimize computational complexity. More fuzzy subsets result in finer control and less oscillation, while increasing the size of memory. The number of fuzzy subset is determined based on the balance of controller performance and the amount of memory used.

C. Rule Base

The rule base is derived from general knowledge of dc–dc converter behavior, and is adjusted based on experimental results. There is a tradeoff between the size of the rule base and the performance of the controller. A 7×7 rule base was also designed and implemented for the buck converter. Experimental results indicated that the fuzzy controller with a 17×17 rule base exhibited less oscillation during steady state and faster transient response was achieved by increasing the output gain h [24]. For the same universe of discourse, more membership functions resulted in finer control. The output of the controller had less variation for small changes in either input, and a more accurate control was achieved; therefore, oscillation in the output voltage and duty cycle was reduced [4].

The nonlinear property of the boost converter's small-signal model, and its right-half-plane zero made the controller design more difficult than for the buck converter. From laboratory experiments, oscillation occurred in steady state when a 17×17 rule base was used for the boost converter. Therefore, a 33×33 rule base was derived for the boost converter in order to obtain fast transient response and reduce steady-state oscillations.

D. Inference Mechanism

The results of the inference mechanism include the weight factor w_i and the change in duty cycle c_i of the individual rule [21]. The weight factor w_i is obtained by Mamdani's min fuzzy implication of $\mu_e(e[k])$ and $\mu_{ce}(ce[k])$, where $w_i = \min\{\mu_e(e[k]), \mu_{ce}(ce[k])\}$ and $\mu_e(e[k])$, $\mu_{ce}(ce[k])$ are the membership degrees [21]. Control c_i is taken from the rule base. The change in duty cycle inferred by the ith rule $z_i = w_i \times c_i$ is given by

$$z_i = \min\left\{\mu_e\left(e[k]\right), \mu_{ce}\left(ce[k]\right)\right\} \times c_i. \tag{16}$$

E. Defuzzification

The center of average method is used to obtain the fuzzy controller's output, which is given in (17), where N is the number of rules that are active [4]

$$\Delta d[k] = \frac{\sum_{i=1}^{N} z_i}{\sum_{i=1}^{N} w_i}. \tag{17}$$

F. Comparison of the Design of PID/PI Controllers to the Design of Fuzzy Controllers

The analysis and design procedure for the linear PID and PI controller are quite different from that for the fuzzy controller in several aspects: design conditions, inputs to the design process, and analysis of design.

1) Design Conditions: Linear controller design is based upon the selection of a single fixed design condition. In this paper, the PID and PI controllers are designed based on nominal operating conditions (input voltage, output voltage, and load). In contrast, design of the fuzzy rule base is a process in which many operating conditions in a 2-D rule space (e, ce) are considered, and a rule for one operating condition can be independently chosen from the rule of a different operating condition.

2) Inputs to the Design Process: Linear controller design begins with a design model of known structure, as described in Section II. For a chosen operating condition, a design model can be derived. On the other hand, design of the fuzzy controller is not based upon a precise mathematical model; fuzzy rules are based upon general knowledge of the converters' dynamic behavior under various operating conditions.

3) Analysis of Design: There are more control design and analysis tools available for PID controllers, and the response is highly predictable for linear plants. Bandwidth, loop gain, and phase margin are the main factors to consider when designing a linear controller based on frequency response techniques. However, because a human's heuristic knowledge is used in the design of fuzzy controllers, there are fewer tools for the design and analysis of fuzzy controllers, and the analysis tends to be more complex. In the absence of expert understanding, extensive tuning is required for the fuzzy controller design process. Computer simulations can provide some guidance and reduce the amount of time needed for tuning.

V. Implementation

Fuzzy controllers for power converters have been implemented using microcontrollers [21], but the computational power of a digital signal processor (DSP) enables higher control sampling frequency [25]. The PID controllers and fuzzy controllers have been implemented and evaluated using a Texas Instruments (TI) eZdsp F2812. The eZdsp F2812 is a standalone evaluation module with a TMS320F2812 DSP, which is a 32-b fixed point DSP controller with on-board Flash memory. The CPU operates at 150 MHz. The TMS320F2812 supports peripherals used for embedded control applications, such as event manager modules and a dual 12-bit, 16 channel ADC. The conversion period of the A/D is 80 ns. The sampling and switching frequency of the PID controllers and the fuzzy controllers was 150 kHz. Since the clock frequency of the DSP is 150 MHz, in order to obtain 10-b resolution of the PWM signal, the switching frequency is chosen to be 150 kHz, and the sampling frequency is chosen to be the same as the switching frequency.

A. Implementation of PID and PI Controllers

The continuous-time transfer function of the PID and PI controllers designed previously were transformed into the discrete-time domain using the backward Euler integration method [26].

The difference equation used to calculate a new duty cycle for the digital PID controller is given by

$$u[k]=K_P e[k]+K_I T\sum_{i=0}^{k} e[k]+\frac{K_D}{T}\left(e[k]-e[k-1]\right). \quad (18)$$

In the difference equation, $u[k]$ is the controller output for the kth sample, and $e[k]$ is the error of the kth sample. The error $e[k]$ is calculated as $e[k] = Ref - ADC[k]$, where $ADC[k]$ is the converted digital value of the kth sample of the output voltage, and Ref is the digital value corresponding to the desired output voltage. The second term on the right side of (18) is the sum of the errors, and third term is the difference between the error of the kth sample and the error of the $(k-1)$ sample. For the PI controller, the derivative gain K_D is set to zero.

The difference equation (18) is a linear combination of feedback and control signals. A series of scalar multiplication and addition instructions can be used to implement the controller. The TI TMS320F2812 DSP is optimized for implementation of digital filters—it has special internal structures to multiply a number by a constant and add the previous product in a single instruction. Therefore, DSP-based implementation of the linear controller in real time is straightforward.

B. Implementation of Fuzzy Controllers

A fuzzy controller is a nonlinear algorithm, which requires frequent use of multiplication and division instructions with high accuracy. There are unique challenges to implement a fuzzy controller on a DSP. When implementing a fuzzy controller in real time, two main issues are the amount of time it takes to compute the output of fuzzy controllers, and the amount of memory used [19].

Between sampling instants, centers in the membership function and their corresponding membership degrees need to be calculated. When there are many inputs to the fuzzy controller, or each input has many membership functions, the efficiency of the implementation of fuzzy controllers becomes even more important, because the number of rules increases exponentially with the increase of the number of inputs. For the fuzzy controller designed for the boost converter, there are two inputs, and each input has 33 membership functions. Therefore, there were totally $33^2 = 1089$ rules. In real time, it was prohibitive to calculate all 1089 membership degrees and to sum up all 1089 values in the numerator and denominator in the center of average method in (17). The sampling frequency of the fuzzy controller would have to be quite low because of the long computation time.

Triangle-shaped membership functions are used to solve this problem. For triangle-shaped membership functions, there are at most four rules that are effective at any time. Therefore, only four centers and four membership degrees need to be calculated instead of going through all the rules in the rule base. The reduction of computation time is significant, particularly when the rule base is large.

The computation time and code size of the fuzzy controller can also be reduced when the number of subsets for the positive and negative parts is a power of two, because shift instructions can be used to calculate the membership degrees instead of division functions. For both converters, initially 17 fuzzy subsets were used with eight positive and negative fuzzy subsets, respectively. From laboratory experiments, oscillation occurred in steady state when 17 fuzzy subsets were used for the boost converter. The fuzzy subsets for the boost converter are increased from 17 to 33 with $2^4 = 16$ positive and negative fuzzy subsets, respectively.

There is a tradeoff between the size of the rule base and the performance of the fuzzy controller. More membership functions result in finer control for the same universe of discourse [4]. However, an increase in the rule base results in a larger amount of memory used. The size of the rule base is determined based on the balance of controller performance and the amount of available memory.

C. Comparison of Implementation of PID and PI Controllers With Implementation of Fuzzy Controllers

Generally, the implementation of a linear controller is less demanding than the implementation of a fuzzy controller. Most DSPs are optimized for implementation of digital filters. On the contrary, more computation power and memory are required to implement a fuzzy controller than a linear controller. To reduce the computation time and amount of memory used, several techniques have been addressed in this effort. A DSP with fast computation speed and high computation power is more appropriate for the implementation of fuzzy controllers in real time. The computation time for the fuzzy controller was 3.6 μs, while the computation time for the PID controller was 1 μs on the TMS320F2812 DSP.

VI. Experimental Results

Experimental results of the buck converter and the boost converter using the PID and PI controllers, and the fuzzy controller are presented and compared in this section. Experimental results including transient responses during startup and load changes under different input voltages are evaluated and compared.

A. Experimental Results of Buck Converter

For the experiment, the prototype buck converter's input voltage was 20 V, the output voltage was 12 V, and the nominal duty cycle was 60%. Startup transient response with input voltage variation from 17 to 23 V was evaluated. Load transient response for 100% load increase (from 0.48 to 0.96 A) and 50% load decrease (from 0.96 to 0.48 A) were also evaluated for various input voltages in the range of 17 to 23 V.

1) Experimental Results of Buck Converter Using PID and PI Control: The startup transient response using the PID/PI controller is shown in Fig. 6(a). The settling time at the nominal input voltage of 20 V was about 4 ms with about 11% overshoot. Both the settling time and overshoot increased when the input voltage increased from 17 to 23 V.

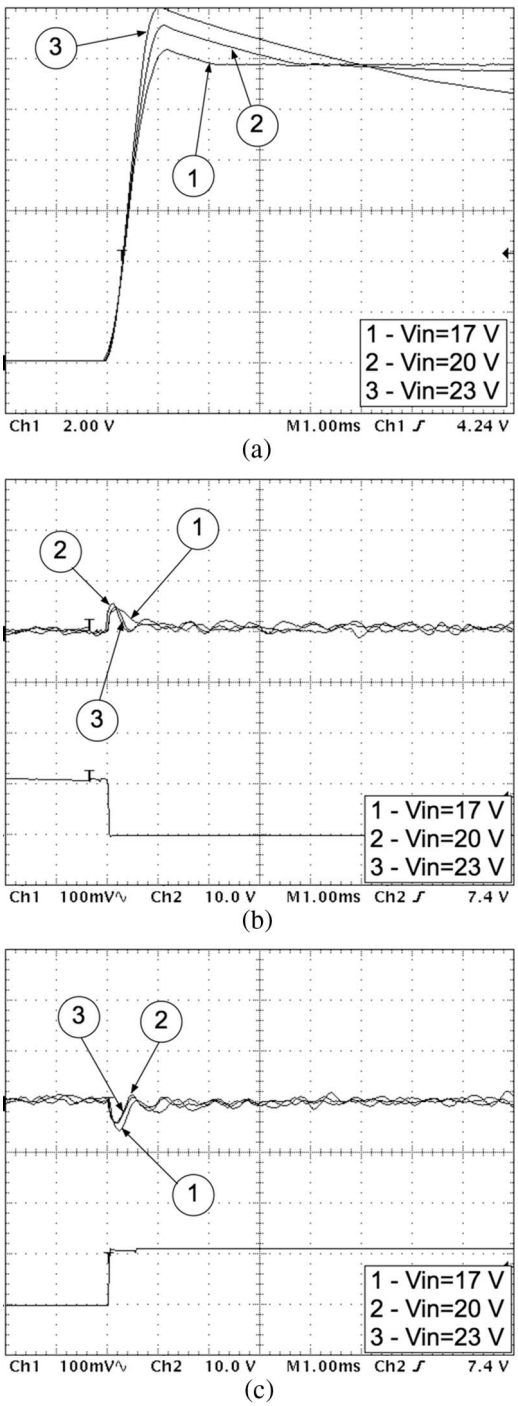

Fig. 6. Buck converter performance under PID/PI control. (a) Startup (2 V/div, 1 ms/div). (b) Load decrease: 50% (100 mV/div, 1 ms/div). (c) Load increase: 100% (100 mV/div, 1 ms/div).

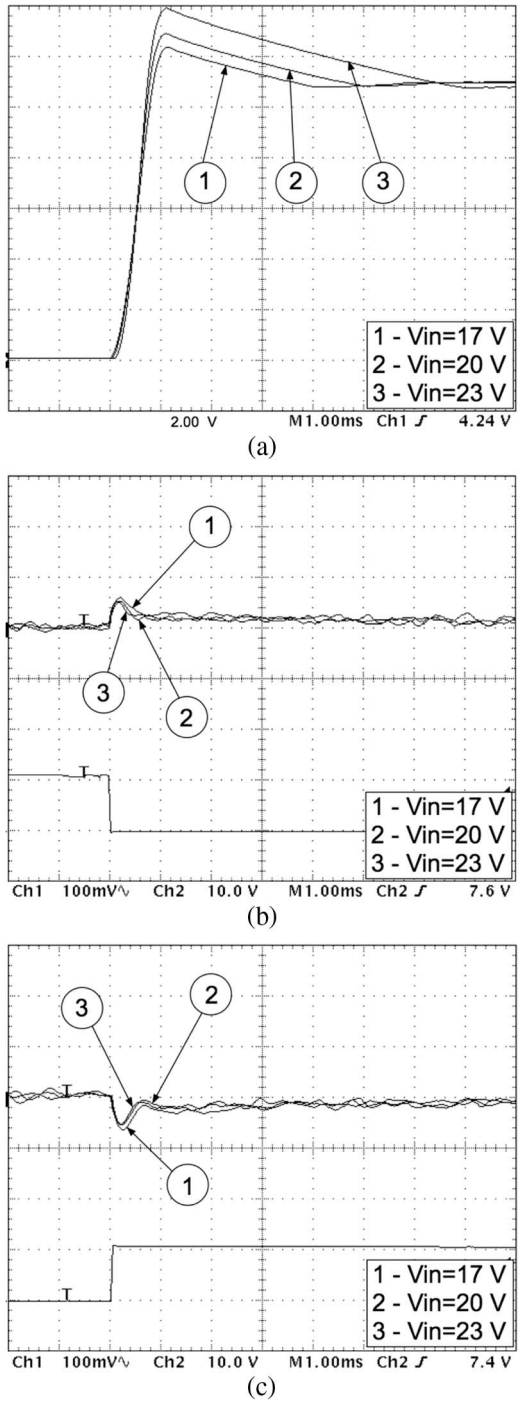

Fig. 7. Buck converter performance under fuzzy control. (a) Startup (2 V/div, 1 ms/div). (b) Load decrease: 50% (100 mV/div, 1 ms/div). (c) Load increase: 100% (100 mV/div, 1 ms/div).

Load transient responses using the PID/PI controller are shown in Fig. 6(b) and (c). In each figure, the upper set of waveforms are the ac coupled voltage responses for different input voltages, and the step waveform underneath is the transient event trigger. Since ac coupling only passes ac signals, it allows a clearer observation of the load transient response. When the load decreased 50% (from 0.96 to 0.48 A), as shown in Fig. 6(b), the settling time remained at about 1 ms, and the maximum transient error remained at about 60 mV for different input voltages. When the load increased 100% (from 0.48 to 0.96 A), as shown in Fig. 6(c), the settling time remained at about 1 ms, and the maximum transient error remained in the range of 40 to 60 mV for different input voltages.

2) Experimental Results of Buck Converter Using Fuzzy Control: The startup transient response when the input voltage varied from 17 to 23 V is shown in Fig. 7(a). The settling time at the nominal input voltage of 20 V was about 6 ms with about 7% overshoot. When the input voltage increased from 17 to 23 V, the settling time remained the same. The overshoot increased when the input voltage increased from 17 to 23 V. The

TABLE III
COMPARISON OF FUZZY CONTROL VERSUS PID AND PI CONTROL FOR BUCK CONVERTER

Performance specification			fuzzy	PID + PI
Startup	Settling time (ms)		6	4
	Overshoot (%)		7	11
Load change	decrease	Settling time (ms)	0.8	1
		Peak error (mV)	60	60
	increase	Settling time (ms)	1	1
		Peak error (mV)	60	40

load transient response of the buck converter using the fuzzy controller when the load current decreased 50% (from 0.96 to 0.48 A) is shown in Fig. 7(b). When the input voltages changed from 17 to 23 V, the settling time remained at about 0.8 ms and maximum transient error remained at about 60 mV. The load transient response of the buck converter when the load current increased 100% (from 0.48 to 0.96 A) is shown in Fig. 7(c). When the input voltage increased from 17 to 23 V, the settling time remained at about 1 ms, and the maximum transient error remained at about 60 mV.

3) Comparison of Experimental Results of the Buck Converter Using PID and PI Controller and Using Fuzzy Controller: A comparison of the performance between the fuzzy control and PID/PI control for the buck converter is quantified in Table III. An examination of the experimental results indicates that the settling time of the startup transient response using fuzzy control is longer than the settling time using PID/PI control, while the overshoot using fuzzy controller is smaller. The startup transient response varied less using fuzzy control than that using PID control. Fuzzy control and PID/PI control obtained very similar load transient response for both load increase and load decrease. When the input voltage changed from 17 to 23 V, the load transient response varied very little.

B. Experimental Results of Boost Converter

For the experiment, the prototype boost converter's input voltage is 5 V, the output voltage is 12 V, and the nominal duty cycle is 58%. Startup transient response with input voltage variation from 4 to 7 V was evaluated. Load transient response for 100% load increase (from 0.24 to 0.48 A) and 50% load decrease (from 0.48 to 0.24 A) were also evaluated for various input voltages in the range from 4 to 7 V.

1) Experimental Results of Boost Converter Using PID and PI Control: The startup transient response using the PID/PI control is shown in Fig. 8(a). The settling time at the nominal input voltage of 5 V was about 25 ms with 8% overshoot. Both the settling time and overshoot decreased as the input voltage increased from 4 to 7 V.

The load transient response of the boost converter using PID/PI control is shown in Fig. 8(b) and (c). When the load decreased 50% from 0.48 to 0.24 A, as shown in Fig. 8(b), the settling time was 10 ms with 240-mV maximum transient error at a nominal input voltage of 5 V. The maximum transient error decreased when the input voltage increased to 6 and 7 V. When the input voltage was reduced to 4 V, there was oscillation in the output voltage. When the load increased 100% (from 0.24 to 0.48 A), as shown in Fig. 8(c), the settling time was 13 ms with 210-mV maximum transient error at a nominal input voltage of 5 V. The response showed underdamped behavior. When the input voltage increased to 6 and 7 V, the settling time decreased and the maximum transient error decreased. When the input voltage was 4 V, there was oscillation in the output voltage.

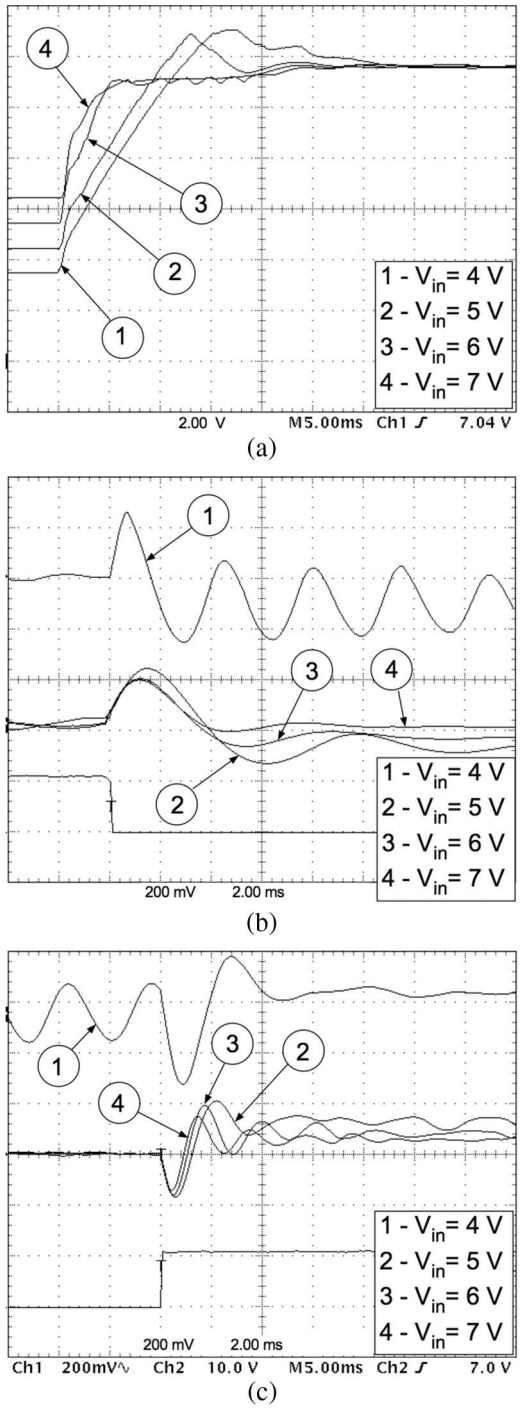

Fig. 8. Boost converter performance under PID/PI control. (a) Startup (2 V/div, 5 ms/div). (b) Load decrease: 50% (200 mV/div, 2 ms/div). (c) Load increase: 100% (200 mV/div, 5 ms/div).

2) Experimental Results of Boost Converter Using Fuzzy Control: The startup transient response of the boost converter using fuzzy control is shown in Fig. 9(a). The settling time was 17 ms with very little overshoot at a nominal input voltage of 5 V. Both the settling time and the overshoot decreased as the input voltage increased from 4 to 7 V.

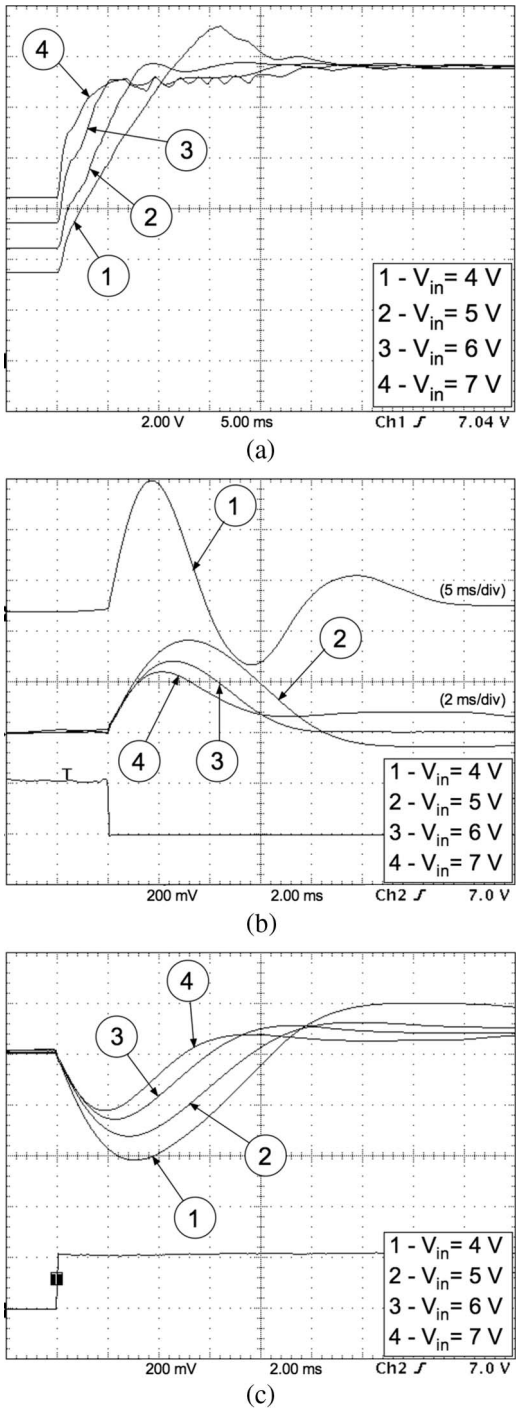

Fig. 9. Boost converter performance under fuzzy control. (a) Startup (2 V/div, 5 ms/div). (b) Load decrease: 50% (200 mV/div, 5 ms/div for curve 1, 2 ms/div for curves 2–4). (c) Load increase: 100% (200 mV/div, 2 ms/div).

The load transient response of the boost converter when the load decreased 50% (from 0.48 to 0.24 A) is shown in Fig. 9(b). At the nominal input voltage of 5 V, the settling time was 10 ms with 360-mV maximum transient error. When the input voltage increased to 6 and 7 V, both the settling time and the maximum transient error decreased. When the input voltage was 4 V, the load transient response exhibited underdamped behavior. The boost converter's load transient response using fuzzy control for a 100% load increase (from 0.24 to 0.48 A) is shown in Fig. 9(c). The settling time was 10 ms with 340-mV maximum transient error. When the input voltage increased from 4 to 7 V, both the settling time and the maximum transient error decreased.

TABLE IV
COMPARISON OF FUZZY CONTROL VERSUS PID AND PI CONTROL FOR BOOST CONVERTER

Performance specification			fuzzy	PID + PI
Startup	Settling time (ms)		17	25
	Overshoot (%)		0	8
Load change	decrease	Settling time (ms)	10	10
		Peak error (mV)	360	240
	increase	Settling time (ms)	10	13
		Peak error (mV)	340	210

3) Comparison of Experimental Results of the Boost Converter Using PID and PI Controller and Using Fuzzy Controller: By comparing the startup transient response of the boost converter in Fig. 8(a) obtained using PID/PI controllers with Fig. 9(a) obtained using fuzzy controllers, it can be observed that the settling time using fuzzy control at nominal input voltage of 5 V was only 17 ms, which was 8 ms less than that using PID/PI control. There was no overshoot at nominal input voltage using fuzzy control, while there was 8% overshoot using PID/PI control. A comparison between the load transient response in Fig. 8(b) obtained using PID/PI control and Fig. 9(b) obtained using fuzzy control when the load decreased 50% (from 0.48 to 0.24 A) indicates that the settling time using fuzzy control at input voltage of 5 V was similar to the settling time using PID/PI control. The maximum transient error using PID/PI control at nominal input voltage was actually lower than that using fuzzy control. When the input voltage was reduced to 4 V, there was oscillation in the output voltage using PID/PI control in Fig. 8(b), while the output voltage was only underdamped using fuzzy control when the input voltage was 4 V. A comparison between the load transient response in Fig. 8(c) obtained using PID/PI control and Fig. 9(c) obtained using fuzzy control when the load increased 100% (from 0.24 to 0.48 A) indicates that by using fuzzy control the load transient response varied less when the input voltage changed from 4 to 7 V. The settling time was also shorter at the nominal input voltage. Although the maximum transient error was smaller using PID/PI control, the output voltage was underdamped during load transient. Furthermore, when using PID/PI control, the output voltage oscillated during load increase when the input voltage was 4 V, while the output voltage does not oscillate using fuzzy control during load increase.

The comparison of the performance between the PID control and fuzzy control for the boost converter is quantified in Table IV. Note that the fuzzy controller is able to achieve faster transient response without overshoot, better rejection to load variation, more stable steady-state response and less dependence on the operating point. An examination of the buck converter and the boost converter's small-signal models suggests that the boost converter's small-signal model is a nonlinear function of the operating point, while only the magnitude of the buck converter's small-signal model shifts with the change of operating point. The PID and PI controller

was designed only for the nominal operating point. When the operating point varied, both the shape and the position of Bode plot of the boost converter's small-signal model changes. Therefore, the linear controller was not able to respond well for the boost converter. On the other hand, since the fuzzy controller does not require an exact mathematical model, it was not designed based on a specific operating point. It responded to the line and load variations more effectively than the linear controller. However, one disadvantage of the fuzzy control method was that it required extensive tuning by the trial and error method.

VII. Conclusion

PID and PI controllers and fuzzy controllers were designed and implemented for both the buck converter and the boost converter. The linear controllers were designed for the converters using frequency response techniques. The PID controller was used for startup transient, while the PI controller was applied during steady state to achieve stable steady-state response. The fuzzy controllers were designed based on an in-depth knowledge of the plant, computer simulations and experimental results. The fuzzy controller for the boost converter used two different controller configurations for the startup transient and for steady state to obtain fast and stable response, while only one configuration was used for the buck converter.

Design and implementation issues and experimental results for the PID and PI controllers and fuzzy controller were compared. The design of linear controllers and fuzzy controllers required quite different procedures. Design of the fuzzy controller did not require a mathematical model, while a small signal model was necessary for the design of PID controllers using frequency response methods. Linear controller design is backed by a long history and wealth of design and analysis tools. More tuning effort was required for fuzzy controllers, and fuzzy control is not a recommended design approach for those who do not have firm grasp or understanding of converter dynamics. Implementation of fuzzy controllers also demanded more computing capability and memory than implementation of linear controllers.

Experimental results showed that fast transient response and stable steady-state responses could be achieved for both the buck and the boost converters using fuzzy controllers. For the buck converter, comparable results were obtained using PID and PI controllers and fuzzy controllers. In other words, it is difficult to justify use of the fuzzy controller for the buck converter, whose dynamics do not change significantly with operating conditions.

In the case of boost converter control, there were some conditions in which the fuzzy control approach yielded superior performance, but there were also some tradeoffs. During startup, the linear and fuzzy control yielded similar responses for most input voltages. In one case, the fuzzy controller yielded less overshoot during the startup transient. Under load changes, the fuzzy controller resulted in less oscillation, but the peak variation was higher in a few cases (decreasing load). In most cases, the fuzzy controller also yielded superior settling time, particularly under load increases.

Acknowledgment

The authors would like to thank the anonymous reviewers for their insightful suggestions.

References

[1] A. Prodic and D. Maksimovic, "Design of a digital PID regulator based on look-up tables for control of high-frequency dc–dc converters," in *Proc. IEEE Workshop Comput. Power Electron.*, Jun. 2002, pp. 18–22.

[2] Y. Duan and H. Jin, "Digital controller design for switchmode power converters," in *Proc. 14th Annu. Appl. Power Electron. Conf. Expo.*, Dallas, TX, Mar. 14–18, 1999, vol. 2, pp. 967–973.

[3] R. P. Severns and G. E. Bloom, *Modern DC-to-DC Switchmode Power Converter Circuits*. New York: Van Nostrand Reinhold, 1985.

[4] K. M. Passino and S. Yurkovich, *Fuzzy Control*. Reading, MA: Addison-Wesley, 1997.

[5] A. Gad and M. Farooq, "Application of fuzzy logic in engineering problems," in *Proc. 27th Annu. Conf. IEEE Ind. Electron. Soc.*, Denver, CO, Nov. 29–Dec. 2, 2001, vol. 3, pp. 2044–2049.

[6] S. Sanchez-Solano, A. J. Cabrera, I. Baturone, F. J. Moreno-Velo, and M. Brox, "FPGA implementation of embedded fuzzy controllers for robotic applications," *IEEE Trans. Ind. Electron.*, vol. 54, no. 4, pp. 1937–1945, Aug. 2007.

[7] S. Chakraborty, M. D. Weiss, and M. G. Simões, "Distributed intelligent energy management system for a single-phase high-frequency ac microgrid," *IEEE Trans. Ind. Electron.*, vol. 54, no. 1, pp. 97–109, Feb. 2007.

[8] G. O. Cimuca, C. Saudemont, B. Robyns, and M. M. Radulescu, "Control and performance evaluation of a flywheel energy-storage system associated to a variable-speed wind generator," *IEEE Trans. Ind. Electron.*, vol. 53, no. 4, pp. 1074–1085, Aug. 2006.

[9] M. Cheng, Q. Sun, and E. Zhou, "New self-tuning fuzzy PI control of a novel doubly salient permanent-magnet motor drive," *IEEE Trans. Ind. Electron.*, vol. 53, no. 3, pp. 814–821, Jun. 2006.

[10] R.-J. Wai and K.-H. Su, "Adaptive enhanced fuzzy sliding-mode control for electrical servo drive," *IEEE Trans. Ind. Electron.*, vol. 53, no. 2, pp. 569–580, Apr. 2006.

[11] P. Mattavelli, L. Rossetto, G. Spiazzi, and P. Tenti, "General-purpose fuzzy controller for dc–dc converters," *IEEE Trans. Power Electron.*, vol. 12, no. 1, pp. 79–86, Jan. 1997.

[12] W.-C. So, C. K. Tse, and Y.-S. Lee, "Development of a fuzzy logic controller for dc–dc converters: Design, computer simulation, and experimental evaluation," *IEEE Trans. Power Electron.*, vol. 11, no. 1, pp. 24–32, Jan. 1996.

[13] C. Cecati, A. Dell'Aquila, A. Lecci, and M. Liserre, "Implementation issues of a fuzzy-logic-based three-phase active rectifier employing only voltage sensors," *IEEE Trans. Ind. Electron.*, vol. 52, no. 2, pp. 378–385, Apr. 2005.

[14] A. G. Perry, G. Feng, Y.-F. Liu, and P. C. Sen, "Design method for PI-like fuzzy logic controllers for dc–dc converter," *IEEE Trans. Ind. Electron.*, vol. 54, no. 5, pp. 2688–2695, Oct. 2007.

[15] Y. Shi and P. C. Sen, "Application of variable structure fuzzy logic controller for dc–dc converters," in *Proc. 27th Annu. Conf. IEEE Ind. Electron. Soc.*, Denver, CO, Nov. 29–Dec. 2, 2001, vol. 3, pp. 2026–2031.

[16] L. Guo, J. Y. Hung, and R. M. Nelms, "Design and implementation of sliding mode fuzzy controllers for buck converters," in *Proc. IEEE Int. Symp. Ind. Electron.*, Montreal, QC, Canada, Jul. 10, 2006, pp. 1081–1087.

[17] K. Viswanathan, R. Oruganti, and D. Srinivasan, "Nonlinear function controller: A simple alternative to fuzzy logic controller for a power electronic converter," *IEEE Trans. Ind. Electron.*, vol. 52, no. 5, pp. 1439–1448, Oct. 2005.

[18] R. W. Erickson and D. Maksimovic, *Fundamentals of Power Electronics*. Norwell, MA: Kluwer, 2001.

[19] L. Guo, R. M. Nelms, and J. Y. Hung, "Comparative evaluation of linear PID and fuzzy control for a boost converter," in *Proc. 31st Annu. Conf. IEEE Ind. Electron. Soc.*, Raleigh, NC, Nov. 2005, pp. 555–560.

[20] M. Smyej, M. Saneba, and A. Cheriti, "A fuzzy controller for a dc to dc converter using a digital integrator," in *Proc. Can. Conf. Elect. Comput. Eng.*, 2000, vol. 1, pp. 7–10.

[21] T. Gupta, R. R. Boudreaux, R. M. Nelms, and J. Y. Hung, "Implementation of fuzzy controller for dc–dc converters using an inexpensive 8-bit microcontroller," *IEEE Trans. Ind. Electron.*, vol. 44, no. 6, pp. 661–669, Oct. 1997.

[22] Y. Shi and P. C. Sen, "Effects of different slopes of membership," in *Proc. 3rd Int. Power Electron. Motion Control Conf.*, Beijing, China, Aug. 2000, pp. 1160–1165.
[23] K.-H. Cheng, C.-F. Hsu, C.-M. Lin, T.-T. Lee, and C. Li, "Fuzzy-neural sliding-mode control for dc–dc converters using asymmetric Gaussian membership functions," *IEEE Trans. Ind. Electron.*, vol. 54, no. 3, pp. 1528–1536, Jun. 2007.
[24] L. Guo, J. Y. Hung, and R. M. Nelms, "Experimental evaluation of a fuzzy controller using a parallel integrator structure for dc–dc converters," in *Proc. IEEE Int. Symp. Ind. Electron.*, Dubrovnik, Croatia, Jun. 20–23, 2005, vol. 2, pp. 707–713.
[25] Z. Z. Ye and M. M. Jovanovic, "Implementation and performance evaluation of DSP-based control for constant-frequency discontinuous conduction mode boost PFC front end," *IEEE Trans. Ind. Electron.*, vol. 52, no. 1, pp. 98–107, Feb. 2005.
[26] C. L. Phillips and R. D. Harbor, *Feedback Control Systems*. Englewood Cliffs, NJ: Prentice–Hall, 1996.

Liping Guo (S'00–M'06) received the B.E. degree in automatic control from Beijing Institute of Technology, Beijing, China, in 1997, and the M.S. and Ph.D. degrees in electrical and computer engineering from Auburn University, Auburn, AL, in 2001 and 2006, respectively.

She is currently an Assistant Professor with the Electrical Engineering Technology Program, Department of Technology, Northern Illinois University, DeKalb. Her research interests are mainly in the area of power electronics, renewable energy sources, embedded systems and control, which include design, modeling, and control of power converters.

Dr. Guo is a member of the IEEE Industrial Electronics Society and Phi Kappa Phi.

John Y. Hung (S'79–M'80–SM'93) received the B.S. degree in electrical engineering from the University of Tennessee, Knoxville, in 1979, the M.S.E. degree in electrical engineering from Princeton University, Princeton, NJ, in 1981, and the Ph.D. degree in electrical engineering from the University of Illinois, Urbana–Champaign, in 1989.

From 1981 to 1985, he was with Johnson Controls, Milwaukee, WI, developing microprocessor-based controllers for commercial heating, ventilation, and air conditioning systems. From 1985 to 1989, he was a Consultant Engineer with Poly-Analytics, Inc. Since 1989, he has been with Auburn University, Auburn, AL, where he is currently a Professor of electrical and computer engineering. His teaching and research interests include nonlinear control systems and signal processing with applications in process control, robotics, electric machinery, and power electronics.

Dr. Hung has received several awards for his teaching and research, including a Best Paper Award from the IEEE TRANSACTIONS ON INDUSTRIAL ELECTRONICS, and two U.S. patents in the area of control systems. He served as an Associate Editor of the IEEE TRANSACTIONS ON CONTROL SYSTEMS TECHNOLOGY (1997, 1998), and the IEEE TRANSACTIONS ON INDUSTRIAL ELECTRONICS (1996–2005). He was the General Chair for the 34th Annual Conference of the IEEE Industrial Electronics Society (IECON-2008). He was Treasurer of the IEEE Industrial Electronics Society (2002–2007) and is currently the IEEE Industrial Electronics Society Vice-President for Conference Activities.

R. M. Nelms (F'04) received the B.E.E. and M.S. degrees in electrical engineering from Auburn University, AL, in 1980 and 1982, respectively, and the Ph.D. degree in electrical engineering from Virginia Polytechnic Institute and State University, Blacksburg, in 1987.

He is currently a Professor and Chair of the Department of Electrical and Computer Engineering, Auburn University. His research interests are in power electronics, power systems, and electric machinery.

Dr. Nelms is a Registered Professional Engineer in the State of Alabama.